Crystal Polymorphism in a Carbamazepine Derivative: Oxcarbazepine

KATIE M. LUTKER, ADAM J. MATZGER

Department of Chemistry, Macromolecular Science and Engineering Program, University of Michigan, Ann Arbor, Michigan 48109-1055

Received 2 March 2009; revised 7 June 2009; accepted 8 June 2009

Published online 14 July 2009 in Wiley InterScience (www.interscience.wiley.com). DOI 10.1002/jps.21873

ABSTRACT: Although crystal polymorphism of carbamazepine (CBZ), an anticonvulsant used to treat epilepsy, has been known for decades, the phenomenon has only recently been noted for its keto-derivative oxcarbazepine (OCB). Here it is demonstrated that OCB possesses at least three anhydrous polymorphs. Although all forms are morphologically similar, making differentiation between crystal modifications by optical microscopy difficult, powder X-ray diffraction, Raman spectroscopy, and thermomicroscopy show distinctive differences. These techniques provide an efficient method of distinguishing between the three polymorphs. The crystal structure of form II of OCB is reported for the first time and the structure of form I has been redetermined at low temperature. Remarkably, both the molecular conformation and crystal packing of form II are in excellent agreement with the blind prediction made in 2007. © 2009 Wiley-Liss, Inc. and the American Pharmacists Association J Pharm Sci 99:794–803, 2010

Keywords: polymorphism; X-ray diffractometry; Raman spectroscopy; crystal structure; calorimetry (DSC)

INTRODUCTION

Polymorphism occurs when a molecule is able to form multiple crystal structures where the packing and/or molecular conformation differs between structures.[1] Although this is far from a universal occurrence in organic compounds,[2] crystal polymorphism has considerable technical importance in industry, especially among pharmaceuticals, where the presence of different structures can affect dissolution rate, solubility, and bioavailability, among other physical characteristics.[1] Despite being highly investigated, the phenomenon of polymorphism continues to present new challenges. In molecular solids, hydrogen bonding and molecular flexibility are thought to be factors contributing to increased propensity towards polymorphism,[3] yet predicting the presence of polymorphic behavior, much less the structure of the polymorphs, remains an outstanding challenge. The conditions under which a crystal is grown clearly affect the crystal structure in polymorphic systems. Recently, insoluble polymers have been utilized to selectively control the crystallization of one polymorph over another.[4] The use of these polymeric heteronuclei has become an efficient and effective tool for screening for polymorphic behavior and the discovery of new polymorphs[4,5] offering the potential to shed light on this fundamental issue in solid-state chemistry. Here we disclose our success in applying polymer-induced heteronucleation to solid form discovery for oxcarbazepine.

Carbamazepine (CBZ) (Fig. 1), an important anticonvulsant, exhibits four structurally characterized polymorphs,[6] whereas its dihydro derivative (10,11-dihydrocarbamazepine) is trimorphic.[7–9] Its keto-derivative, oxcarbazepine (OCB) (Fig. 1), also used as an anticonvulsant,

Correspondence to: Adam J. Matzger (Telephone: 7346156627; Fax: 7346158553; E-mail: matzger@umich.edu)

Journal of Pharmaceutical Sciences, Vol. 99, 794–803 (2010)

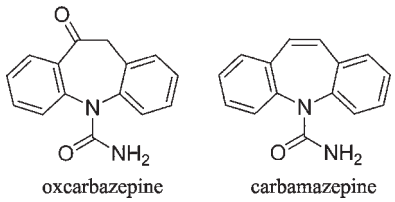

Figure 1. Molecular structures of carbamazepine (left) and oxcarbazepine (right).

is believed to also be polymorphic and patent literature claims a total of five polymorphs and a solvate albeit with levels of characterization inadequate to prove that these are novel forms.[10,11] The characterization of three anhydrous polymorphs is reported herein. The commercially available form I crystallizes in the monoclinic space group $P2_1/c$, with cell constants of $a = 5.276(2)$ Å, $b = 9.307(4)$ Å, $c = 24.841(7)$ Å, and $\beta = 95.64(2)$ °.[12] The possibility of other structures for OCB has been suggested by computational studies,[13] although these have yet to realize experimental verification. One form proposed by Cabeza et al. appears to have a similar powder X-ray diffraction pattern to that of a form suggested in the patent literature.[10,11] The present study reveals two additional forms of OCB, including one that matches the prediction of Cabeza et al., making it, at least, a trimorphic system. This observation contributes to the mounting evidence that the basic backbone of carbamazepine and urea functionality constitute a polymorphophore.[14]

The two newly discovered forms of OCB reported herein, form II and form III, along with form I have been characterized by Raman spectroscopy, differential scanning calorimetry (DSC), thermomicroscopy, and powder X-ray diffraction (PXRD). The structure of form I was redetermined at low temperature. The crystal structure of form II was solved and found to be in good agreement with that predicted by Cabeza et al.[13]

EXPERIMENTAL

Materials

Commercial OCB was obtained from Orgamol (Evionnaz, Switzerland). Toluene (ACS grade) and methanol (ACS grade) were purchased from Fisher Scientific (Pittsburgh, PA). Ethylene/vinyl acetate copolymers and high-density polyethylene were purchased from Scientific Polymer Products, Inc. (Ontario, NY).

Preparation of OCB Polymorphs

Form I of OCB was obtained directly from the bottle and from the evaporation of a methanol solution. Various concentrations were used, with higher concentrations yielding larger, better quality crystals. Form II was produced by dissolving 25.0 mg of OCB in 20 mL of toluene and heating the solution to 115°C until homogeneous. The solution was then allowed to cool to room temperature or placed in an ice bath until crystals were formed. The small needles (in most cases more powder-like than individual crystals) were collected after about an hour. Seeding of supersaturated toluene solutions (2.5 mg/mL) of oxcarbazepine at room temperature with form II seeds consistently yielded bulk form II, whereas the cooling of the solution alone yielded either form I or form II. Form III was obtained through the evaporation of methanol solutions (5 mg/mL) in the presence of ethylene/vinyl acetate copolymers or high-density polyethylene at room temperature.

Powder X-Ray Diffraction

PXRD patterns were obtained on a Bruker D8 Advance diffractometer operating at 40 kV and 40 mA with a copper source between 3 and 50° 2θ with a step size of 0.020°. The step time for forms I and II was 5 s and that for form III was 30 s. Samples were measured directly on a glass slide at room temperature.

Single Crystal X-Ray Diffraction

All measurements were made on a Rigaku R-AXIS SPIDER diffractometer with an image plate detector using graphite monochromated Cu-Kα radiation (1.5406 Å). The data collection was made at 95 K with the sample mounted on a MiTeGen MicroMount™. The structure was solved by direct methods.[15] All calculations were performed using the CrystalStructure crystallographic software package[16] except for refinement, which was performed using SHELXL-97.[17]

Raman Spectroscopy

Raman spectra were recorded on a Renishaw inVia Raman Microscope equipped with a 20× objective and utilizing a 633 nm HeNe laser. The scan range was 3600–100 cm^{-1} using three scans of length 60 s per spectrum. A silicon standard was used to calibrate the instrument.

Infrared Spectroscopy

IR spectra were obtained with a Perkin-Elmer AutoIMAGE FTIR microscopy system in transmission mode using 100 scans per spectrum.

Thermomicroscopy

A Mettler Toledo FP82HT hot stage using an FP90 control processor was used for thermomicroscopy. The sample was observed under polarized light with a Leica DMLP microscope. Samples were heated from 30 to 220°C at a rate of 5°C/min. Forms II and III were also heated until each fully transformed and then allowed to cool. The transformation product was then identified using Raman spectroscopy and/or PXRD.

Differential Scanning Calorimetry

DSC was performed on a TA Instruments DSC Q10. Samples were placed in aluminum hermetic pans and sealed using a TA Instruments crimper. The temperature range was 20–300°C with a heating rate of 10°C/min.

RESULTS AND DISCUSSION

PXRD

PXRD is a particularly diagnostic way of differentiating between OCB polymorphs. Form I has characteristic peaks at $2\theta = 10.36$, 12.10, and 14.43°. Form II has a greater number of intense peaks than form I and can be distinguished by those at $2\theta = 11.82$, 14.22, 18.20, 21.79, and 24.60°. Form III is easily identifiable by the presence of a relatively low angle peak at 4.95° 2θ and other prominent peaks at 8.58, 11.98, 13.08, and 19.78° 2θ. Table 1 lists all the peaks and their relative intensities and Figure 2 presents the powder patterns.

Table 1. Powder X-Ray Diffraction Peak Positions and Relative Intensities for the Polymorphs of OCB

Form I		Form II		Form III	
2θ (°)	Intensity (%)	2θ (°)	Intensity (%)	2θ (°)	Intensity (%)
7.36	5.0	7.14	55.2	4.95	100.0
10.36	12.2	11.82	36.6	8.58	74.7
11.96	81.0	14.22	100.0	11.98	27.3
12.10	100.0	17.06	8.5	13.08	89.6
14.43	21.2	17.87	7.3	14.34	15.6
14.54	32.3	18.20	90.0	19.12	12.6
17.39	2.8	18.76	60.1	19.78	34.1
17.84	1.2	19.48	41.9		
19.10	7.7	20.11	1.9		
19.27	12.4	20.49	6.6		
19.60	6.6	21.18	3.5		
20.19	3.7	21.79	42.5		
21.28	1.9	22.69	4.2		
22.12	3.9	23.40	13.0		
23.13	4.7	23.81	6.4		
23.24	6.0	24.60	34.7		
23.78	17.2	25.42	10.3		
24.12	2.8	26.22	4.9		
25.36	4.1	26.87	13.2		
25.68	5.9	28.00	6.2		
25.76	6.3	28.54	2.0		
26.28	2.8	29.60	7.6		
29.88	5.2	32.90	2.8		
41.49	2.8	34.15	2.6		
		35.79	2.8		
		36.14	1.8		
		38.06	9.0		
		44.55	2.8		

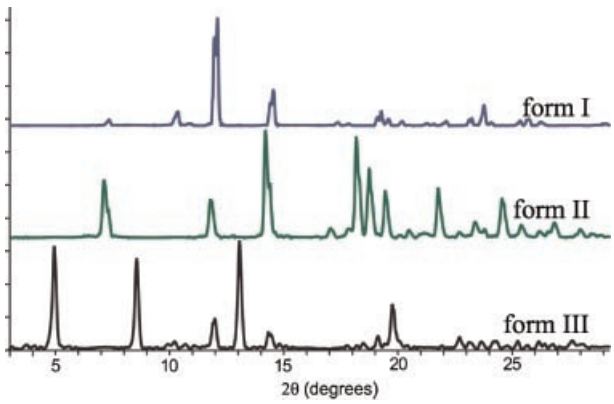

Figure 2. PXRD patterns of the three polymorphs of OCB.

DOI 10.1002/jps

Raman Spectroscopy

Although the Raman spectra of forms I and II are very similar, they possess several regions where they can be differentiated. The characteristic areas where all three polymorphs are easily discriminated from one another are 100–200, 700–800, 1100–1300, 1500–1700, and 2900–3400 cm^{-1}. For form I, peaks occur at 162.3, 776.7, 1154.3, 1262.4, 1270.6, and 1570.3 cm^{-1}. The corresponding peaks in Form II are 159.5, 778.0, 1152.9, 1259.5, 1272.0, and 1568.9 cm^{-1}. The spectrum for form III differs significantly from those of forms I and II, making Raman spectroscopy an efficient method for its identification. Form III has corresponding peaks at 155.4, 779.4, 1154.3, 1258.1, 1276.1, and 1594.9 cm^{-1}. Significant differences are also observed in the hydrogen bonding region between 2900 and 3600 cm^{-1}. Here it can be observed that forms I and II have a similar hydrogen bonding motif within their crystal structure (see below), whereas form III is different as evidenced by the missing peak around 3340 cm^{-1}. Forms I and II also each have a peak around 3470 cm^{-1} that is shifted to 3340 cm^{-1} in the spectrum of form III. A complete list of peaks is shown in Table 2 and the spectra are presented in Figure 3.

Infrared Spectroscopy

The IR spectra reveal the structural similarities and disparities between the polymorphs. From the spectra it can be concluded that the hydrogen bonding scheme exhibited by forms I and II are very similar. Form III has a different hydrogen bonding motif. In forms I and II the hydrogen bonding motif can be attributed to peaks at about 3471 and 3345 cm^{-1}, while in form III a significant shift and the addition of one peak is observed (3303, 3353, and 3435 cm^{-1}). Other major differences occur in the carbonyl region that can be attributed to the hydrogen bonding present in the crystal structure. In this region the peak that is at 1734 cm^{-1} in form I and 1733 cm^{-1} in form II disappears entirely from the spectrum of form III. Another significant dissimilarity is between 900 and 1000 cm^{-1}. Form I has peaks at 923, 956, and 985 cm^{-1}, while form II has peaks at 922, 959, and 994 cm^{-1} and form III has peaks at 922, 949, 968, and 997 cm^{-1}. The IR spectra are shown in Figure 4 and the peak data are tabulated in Table 3.

Thermomicroscopy/DSC

The behavior of oxcarbazepine during heating was observed on a hot stage (5°C/min) under crossed polarizers. No transitions were observed in form I before it melted. The DSC curve of form I showed an endotherm (melt/decomposition) with an onset of 222.6°C at a rate of 10°C with an enthalpy of 9.64 kcal/mol. Thermomicroscopy proved that for all polymorphs melting and decomposition occurred simultaneously and this contributes to the large melting range measured. During decomposition the melt turns from colorless to yellow. The decomposition of oxcarbazepine is dependent upon the crystal size, with smaller and more defective crystals decomposing before larger ones.

A transition between 118 and 150°C was observed during the heating of form II. The temperature of this transition is highly dependent on crystal size and quality, with smaller crystals having more defects observed to transform before larger more perfect crystals. The DSC thermogram for form II exhibited an endothermic transition centered at 127.6°C followed immediately by a broad exothermic transition centered at 165.8°C. The approximate enthalpy of the endotherm is 0.23 kcal/mol while that of the exotherm was 0.42 kcal/mol. The endotherm is somewhat less than the predicted energy difference of 0.61 kcal/mol separating calculated form I and the next most stable form of Cabeza et al.[13] The ensuing melt/decomposition has an onset of 218.2°C with an enthalpy of 7.97 kcal/mol. In order to determine which modification form II transformed into during heating, a sample was heated to 160°C and held there for 5 min. The sample was allowed to cool to room temperature. Raman microscopy and PXRD was performed on the product, which proved to be form I.

Form III showed a small transition between 115 and 125°C. The melt occurs between 210 and 216°C. The thermogram of form III shows a large endothermic transition between 58 and 150°C with a melt/decomposition onset of 210.0°C. The enthalpy of the transition is 6.23 kcal/mol. To determine which polymorph form III had transformed into, a sample was heated to 150°C and held there for 5 min. Upon cooling to room temperature, the sample was found to be form I by Raman microscopy. In all of the polymorphs the melt was concomitant with decomposition. The DSC thermograms are presented in Figure 5.

Table 2. Summary of Raman Peak Positions for the Three Polymorphs of OCB

Raman Shift (cm^{-1})	Form I	Form II	Form III
100–200	3 peaks at 134.9, 162.3, and 186.9	2 peaks at 159.5 with shoulder at 134.9 and 184.2	2 peaks at 155.4 with shoulder at 124.0 and 182.8
200–300	1 peak at 266.3	1 peak at 263.5	2 peaks at 259.4 and 269.0
300–400	4 peaks at 310.1, 330.6, 362.1, and 378.5	3 peaks at 310.1, 329.2, and 360.7 with shoulder at 375.7	3 peaks at 314.2, 330.6, and 362.1 with shoulder at 377.1
400–500	2 peaks at 418.2 with shoulder at 425.0 and 453.7	2 peaks at 418.2 and 452.4	2 peaks at 429.1 and 457.8
500–600	2 peaks at 515.3 and 553.6	2 peaks at 513.9 and 552.2	3 peaks at 511.2, 555.0, and 598.8
600–700	4 peaks at 612.5 with shoulder at 598.8, 652.1, 668.6, and 698.7	4 peaks at 612.0 with shoulder at 601.0, 652.1, 667.2, and 697.3	3 peaks at 622.0, 650.8, and 671.3
700–800	3 peaks at 743.8, 753.4 with shoulder at 758.9, and 776.7	2 peaks at 743.8 and 778.0	5 peaks at 700.0, 742.4, 756.1, 767.1, and 779.4
800–900	2 peaks at 845.1 and 886.1	3 peaks at 846.4, 882.0, and 888.9	2 peaks at 842.3 and 872.4
900–1000	3 peaks at 924.4, 950.4, and 962.7	3 peaks at 923.1, 950.4, and 966.8	2 peaks at 923.1 and 950.4
1000–1100	2 peaks at 1016.1 with shoulders at 987.4, 1031.2, and 1055.8	3 peaks at 1014.7 with shoulder at 994.2, 1038.0, and 1055.8	3 peaks at 1016.1 (broad) with shoulder at 998.3, 1039.4, and 1053.1
1100–1200	3 peaks at 1107.8, 1154.3 with shoulder at 1163.8, and 1194.0	3 peaks at 1106.4, 1152.9 with shoulder at 1165.3, and 1192.6	3 peaks at 1103.7 with shoulder at 1117.3, 1154.3, and 1191.3
1200–1300	2 peaks 1237.8 and 1262.4 with shoulder at 1270.6	3 peaks at 1237.8, 1259.7, and 1272.0	5 peaks at 1244.6, 1258.3, 1276.1, 1287.0, and 1298.0 (broad) with shoulders at 1306.5 and 1317.1
1300–1400	1 peak at 1303.5 (broad) with shoulder at 1324.0	1 peak at 1300.7 (broad) with shoulder at 1321.2	0 peaks
1400–1500	3 peaks at 1423.9 with shoulder at 1406.1, 1451.2, and 1477.2 with shoulder at 1490.9	3 peaks at 1406.1, 1451.2, and 1477.2 with shoulder at 1491.3	3 peaks at 1419.8, 1451.2, and 1477.2
1500–1600	2 peaks at 1570.3 and 1597.6 with shoulder at 1586.7	2 peaks at 1568.9 and 1597.6 with shoulder at 1587.4	3 peaks at 1523.8, 1571.6 and 1594.9 with shoulder at 16-07.2
1600–1700	2 peaks at 1653.7 and 1681.1	2 peaks at 1655.1 and 1681.1	2 peaks at 1645.5 and 1675.6 with shoulder at 1683.8
2500–2600		1 peak at 2599.3	1 peak at 2597.9
2800–2900	1 peak at 2820.9	1 peak at 2814.1	1 peak at 2819.6
2900–3000	2 peaks at 2909.9 and 2986.5	2 peaks at 2909.9 and 2975.5 with shoulder at 2986.5	2 peaks at 2911.2 and 2986.5
3000–3100	4 peaks at 3004.3, 3042.6 with shoulder at 3033.0, and 3076.8 with shoulder at 3063.1	4 peaks at 3005.6, 3018.0, 3042.6, and 3073.6 with shoulder at 3065.2	4 peaks at 3005.6, 3037.1 with shoulder at 3039.9, 3061.8, and 3085.0
3100–3200	1 peak at 3142.5	3 peaks at 3141.1, 3171.2, and 3193.1	3 peaks at 3141.1, 3168.5, and 3187.6
3300–3400	1 peak at 3345.0	1 peak at 3342.3	0 peaks
3400–3500	1 peak at 3473.6	1 peak at 3475.0	1 peak at 3440.8

 DOI 10.1002/jps

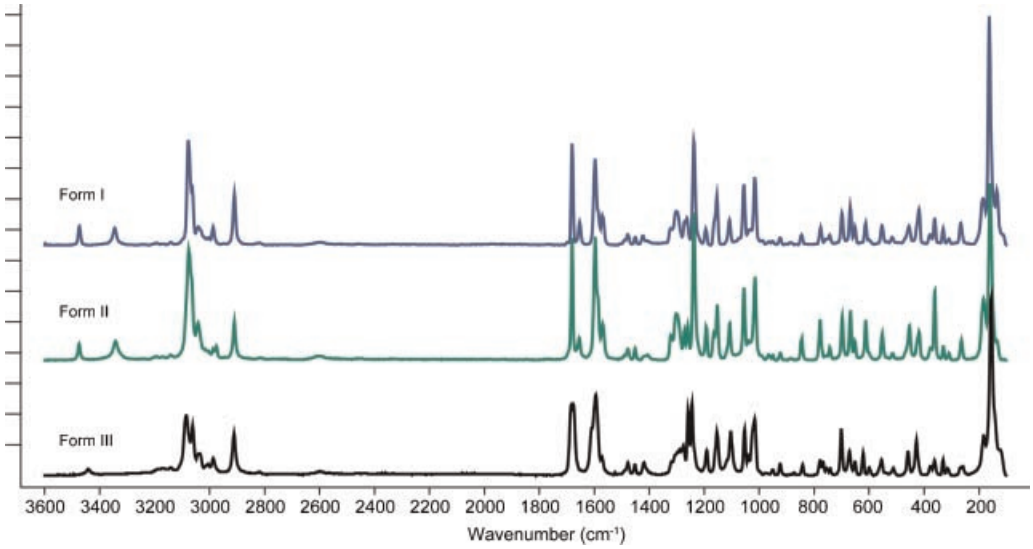

Figure 3. Raman spectra of the three polymorphs of OCB.

Single Crystal X-Ray Diffraction

The crystal structure of form I was re-determined at low temperature and that of form II was solved for the first time (Tab. 4, Figs. 6 and 7). The molecular conformation in forms I and II are similar. In form I, the azepine ring is in a twist-boat conformation. The angle between the planes defined by the benzene rings is 63°. The carboxamide group is extended above the rest of the molecule and participates in hydrogen bonding directed by the carbonyl of the carboxamide group on one molecule binding with the hydrogen of the NH_2 of next molecule creating infinite chains along the *b*-axis. The length of the hydrogen bond ($O \cdots N$) is 2.77 Å. This differs dramatically from the anti-hydrogen bonded dimers observed in the four polymorphs of carbamazepine.[6] The second hydrogen in the carboxamide functionality participates in $N - H \cdots \pi$ bonding with the benzene ring nearest to it. In addition to hydrogen bonding, $C - H \cdots O$ interactions are present between the carbonyl of the azepine ring and a hydrogen on a benzene ring of a neighboring molecule thus creating dimers and connecting adjacent hydrogen bonded chains. As pointed out previously,[13]

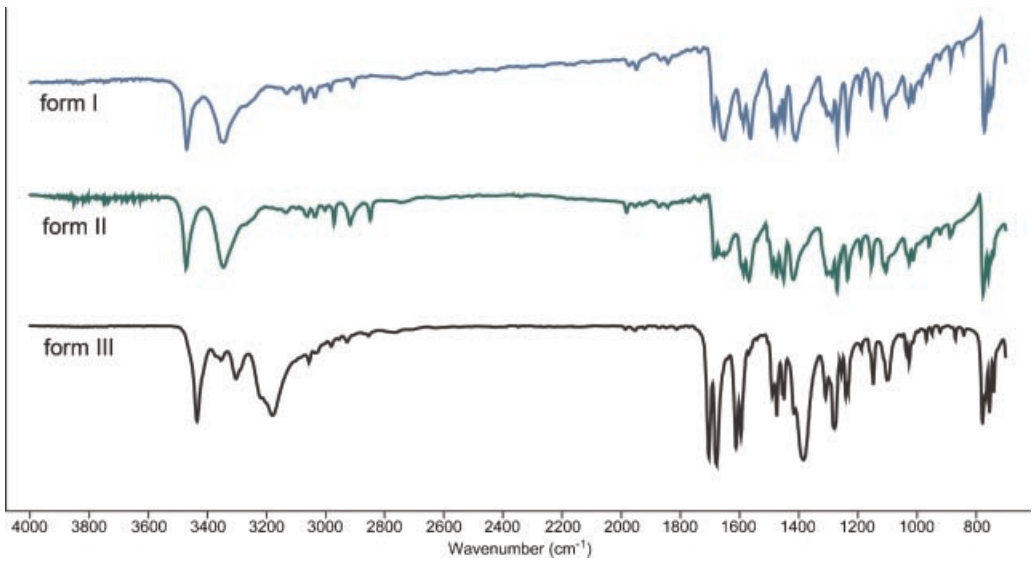

Figure 4. Infrared spectra of forms I, II, and III of oxcarbazepine.

Table 3. Summary of IR Peak Positions for the Three Polymorphs of OCB

Wavenumber (cm^{-1})	Form I	Form II	Form III
700–800	4 peaks at 743, 750, 758, and 771	4 peaks at 742, 751, 758, and 776	4 peaks at 740, 754, 767, and 778
800–900	2 peaks at 846 and 885 with shoulder at 876	2 peaks at 847 and 888 with shoulder at 880	2 peaks at 841 and 870
900–1000	3 peaks at 923, 956, and 985	3 peaks at 922, 959 with shoulder at 948, and 994	4 peaks at 922, 949, 968 with shoulder at 977, and 997
1000–1100	2 peaks at 1013 and 1027 with shoulder at 1035	2 peaks at 1012 and 1026 with shoulder at 1035	3 peaks at 1026 with shoulder at 1014, 1036, and 1052
1100–1200	3 peaks at 1104 with shoulder at 1074, 1154, and 1192	3 peaks at 1105 with shoulder at 1114, 1153, and 1190	1 peak at 1101 (broad) with shoulder at 1159
1200–1300	3 peaks at 1235, 1269, and 1287 with shoulder at 1304	4 peaks at 1235, 1257, 1270, and 1287 with shoulder at 1295	5 peaks at 1233, 1241, 1255, 1277, and 1283 with shoulder at 1293
1300–1400	1 peak at 1313 with shoulder at 1321	1 peak at 1304	2 peaks at 1309 and 1384 (broad) with shoulder at 1417
1400–1500	5 peaks at 1410 with shoulder at 1372, 1448, 1459, 1474, and 1489 with shoulder at 1505	4 peaks at 1418 with shoulder at 1373, 1451 with shoulder at 1458, 1474, and 1489 with shoulder at 1505	4 peaks at 1449, 1456, 1474, and 1489 with shoulder at 1505
1500–1600	3 peaks at 1564, 1586, and 1595	4 peaks at 1539, 1568, 1587, and 1595	4 peaks at 1540, 1560, 1568, and 1595
1600–1700	2 peaks at 1652 and 1686	2 peaks at 1652 with shoulder at 1646 and 1661 and 1687 with shoulder at 1680	3 peaks at 1612, 1641, and 1678
1700–1800	3 peaks at 1716, 1734, and 1771	3 peaks at 1716, 1733, and 1771	3 peaks at 1703, 1771, and 1791
1800–1900	2 peaks at 1843 and 1867	2 peaks at 1843 and 1873	3 peaks at 1813, 1848, and 1875
1900–2000	2 peaks at 1949 and 1974	3 peaks at 1928, 1952, and 1982	3 peaks at 1921, 1953, and 1986
2800–2900		1 peaks at 2849	1 peak at 2855 with shoulder at 2871
2900–3000	3 peaks at 2907, 2949, and 2984	2 peaks at 2917 and 2971	1 peaks at 2956 and 2981
3000–3100	5 peaks at 3001, 3014, 3037, 3070, and 3099	4 peaks at 3002, 3036, 3062, and 3098	2 peaks at 3037 with shoulder at 3029 and 3056
3100–3200	2 peaks at 3131 and 3163	1 peak at 3136	1 peaks at 3180 with shoulder at 3219
3300–3400	1 peak at 3343 with shoulder at 3272	1 peak at 3346 with shoulder at 3272	2 peaks at 3303 and 3353 with shoulder at 3370
3400–3500	1 peak at 3470	1 peak at 3472	1 peak at 3435

form I oxcarbazepine is isostructural to form I of dihydrocarbamazepine.

The experimental crystal structure of form II is very similar to the second lowest energy predicted structure from Cabeza et al.[13] The molecular conformation of form II is related to form I. The benzene rings are planar and the angle between the planes is 65°. Consistent with the vibrational spectroscopy, the carboxamide group adopts a hydrogen bonding scheme similar to that in form I with infinite chains parallel to the *b*-axis. The hydrogen bond ($O \cdots N$) distance is 2.75 Å. Unlike form I, the hydrogen of the amide that does not participate in strong hydrogen bonding forms $N - H \cdots \pi$ interactions. A major difference between the structures of form I and form II is the nature of the $C - H \cdots O$ interactions. Instead of the dimers observed in form I, the carbonyl of the azepine ring interacts with two separate molecules from an adjacent chain, thus linking two different chains.

The structure of form III was never determined due to the small size and poor quality of the crystals. Crystal size and quality were unable to be improved upon, despite adjusting crystallization parameters and attempting seeding. The packing

Table 4. Cell Parameters for Forms I and II

	Form I	Form II
Crystal system	Monoclinic	Monoclinic
Space group	$P2_1/c$	$P2_1$
Unit cell		
a	5.20194(16) Å	5.1606(2) Å
b	9.2638(3) Å	9.4057(4) Å
c	24.7989(7) Å	12.5984(5) Å
α	90°	90°
β	95.234(2)°	92.720(3)°
γ	90°	90°
Volume	1190.07	610.825
Z	4	2
Density	1.408 g/cm^3	1.372 g/cm^3
Crystal size	0.20 × 0.07 × 0.06 mm	0.15 × 0.03 × 0.01 mm
Goodness of fit	1.017	1.040
Final R indices (obs data) [$I > 2\sigma(I)$]	0.0404	0.1280
Final R indices (all data)	0.0465	0.1954
wR	0.0905	0.3024

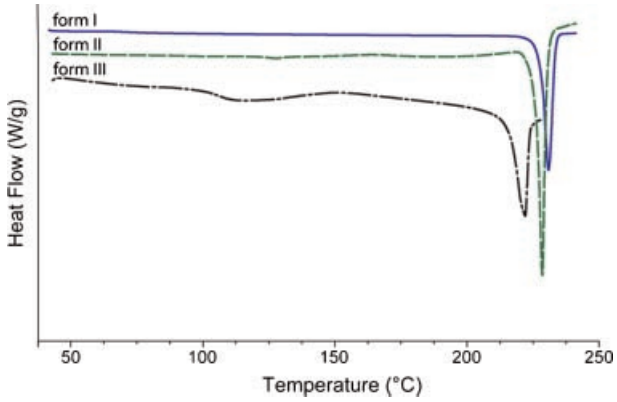

Figure 5. DSC thermographs of the three polymorphs of OCB.

motif observed in forms I and II of oxcarbazepine differs greatly from that seen in carbamazepine and some of its other derivatives. One major difference from carbamazepine is the asymmetry of azepine ring in OCB. This leads to a greater puckering of the azepine ring on one side of the molecule. This is thought to allow for the optimization of the hydrogen bonding in a chain motif.[13] All three structures of dihydrocarbamazepine also exhibit an analogous hydrogen bonding scheme to OCB, as they all form hydrogen bonded chains.[7–9] The hydrogen bonding in all four of the carbamazepine polymorphs favor an anti-dimer motif,[6] whereas the structure of epoxycarbamazepine displays a twisted syn-dimer configuration.[18] In contrast to carbamazepine, dihydrocarbamazepine form I is almost isostruc-

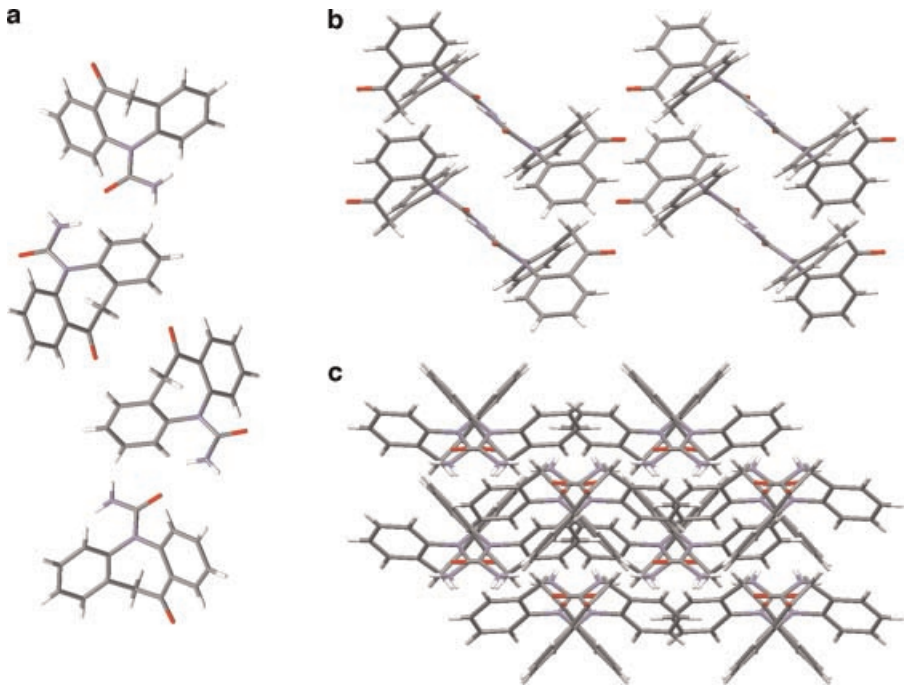

Figure 6. Unit cell of form I. (a) View down a-axis, (b) view down b-axis, (c) view down c-axis.

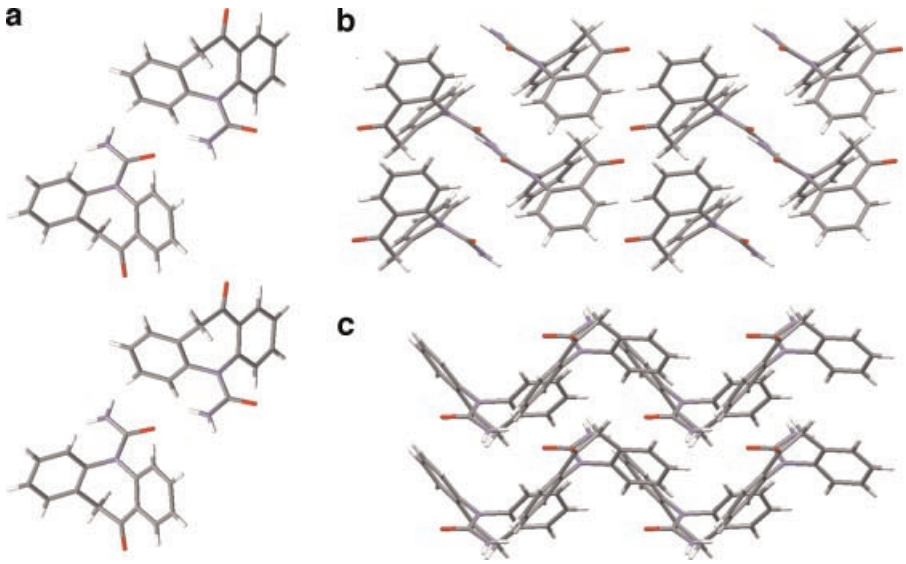

Figure 7. Unit cell of form II. (a) View down *a*-axis, (b) view down *b*-axis, (c) view down *c*-axis.

tural to OCB form I and exhibits a similar conformation of the azepine ring.[13] Hydroxycarbamazepine, although similar to OCB and epoxycarbamazepine in the fact that it adds an additional functional group that can participate in hydrogen bonding, differs from these structures as it actually hydrogen bonds through the alcohol in addition the carboxamide functionality and thus forms neither anti-dimers nor chains.[19]

CONCLUSION

OCB is at minimum trimorphic and two of these forms are structurally characterized. While the crystal structure for form III remains elusive, the presence of this form has been confirmed through multiple methods. The packing motif for forms I and II differ from those observed in the polymorphs of carbamazepine. This shows that although the basic molecular structure of carbamazepine and oxcarbazepine are similar, the change from a double bond bridge to an alkyl carbonyl is significant in the packing of the molecules. Because oxcarbazepine, dihydrocarbamazepine, and carbamazepine are polymorphic, the basic backbone of the molecules should be considered a polymorphophore.[14] Additional work is needed to verify all of the polymorphic forms reported in the patent literature.[10,11]

REFERENCES

1. Brittain HG. 1999. Polymorphism in pharmaceutical solids. 1st editon. New York: Marcel Dekker.
2. Gavezzotti A, Filippini G. 1995. Polymorphic forms of organic-crystals at room conditions—Thermodynamic and structural implications. J Am Chem Soc 117:12299–12305.
3. Yu L, Reutzel-Edens SM, Mitchell CA. 2000. Crystallization and polymorphism of conformationally flexible molecules: Problems, patterns, and strategies. Org Process Res Dev 4:396–402.
4. Lang MD, Grzesiak AL, Matzger AJ. 2002. The use of polymer heteronuclei for crystalline polymorph selection. J Am Chem Soc 124:14834–114835.
5. Price CP, Grzesiak AL, Matzger AJ. 2005. Crystalline polymorph selection and discovery with polymer heteronuclei. J Am Chem Soc 127:5512–5517.
6. Grzesiak AL, Lang MD, Kim K, Matzger AJ. 2003. Comparison of the four anhydrous polymorphs of carbamazepine and the crystal structure of form I. J Pharm Sci 92:2260–2271.
7. Bandoli G, Nicolini M, Ongaro A, Volpe G, Rubello A. 1992. X-ray crystallographic characterization of 10,11-dihydro-5H-dibenz[b,f]azepine-5-carboxamide. J Crystallogr Spectrosc Res 22:177–183.
8. Harrison WTA, Yathirajan HS, Anilkumar HG. 2006. An orthorhombic polymorph of 10,11-dihydrocarbamazepine. Acta Crystallogr C 62:240–242.
9. Leech CK, Florence AJ, Shankland K, Shankland N, Johnston A. 2007. 10,11-dihydrocarbamazepine (form III). Acta Crystallogr E 63:675–677.

10. Aronhime J, Dolitzky B-H, Berkovich Y, Garth N. Crystal forms of oxcarbazepine and processes for their preparation. US7183272 (published on February 27, 2007).
11. Venkataraman S, Raju NS, Purandhar K, Reddy LA, Kondaiah GCM. Crystalline form of oxcarbazepine. US20060166968 (published on July 15, 2005).
12. Hempel A, Camerman N, Camerman A, Mastropaolo D. 2005. Oxcarbazepine: Structure and anticonvulsant activity. Acta Crystallogr E 61:1313–1315.
13. Cabeza AJC, Day GM, Motherwell WDS, Jones W. 2007. Importance of molecular shape for the overall stability of hydrogen bond motifs in the crystal structures of various carbamazepine-type drug molecules. Cryst Growth Des 7:100–107.
14. Lutker KM, Tolstyka ZP, Matzger AJ. 2008. Investigation of a priveleged polymorphic motif: A dimeric ROY derivative. Cryst Growth Des 8:136–139.
15. Burla MC, Caliandro R, Camalli M, Carrozzini B, Cascarano GL, De Caro L, Giacovazzo C, Polidori G, Spagna R. 2005. SIR2004: An improved tool for crystal structure determination and refinement. J Appl Crystallogr 38:381–388.
16. 2000-2005. CrystalStructure 3.7.0 ed. ed., The Woodlands, TX 77381: Rigaku and Rigaku/MSC. p Crystal Structure Analysis Package.
17. Sheldrick GM. 1997. SHELXS97 and SHELXL97. Germany: University of Gottingen.
18. Bellucci G, Cinzia C, Marchetti F. 1995. Conformational process and symmetry in N-substituted 10,11-dihydro-5H-dibenz[b,f]azepine and 1a,10b-dihydro-6H-dibenzo[b,f]oxireno[d]azepine Derivatives. Gazz Chim Ital 125:341–346.
19. Lisgarten JN, Palmer RA, Saldanha JW. 1989. The structure of 10,11-dihydro-10-hydroxy-5h-dibenz[B,F] azepine-5-carboxamide, an anticonvulsant drug molecule. Acta Crystallogr C 45:656–658.